Accepted Manuscript

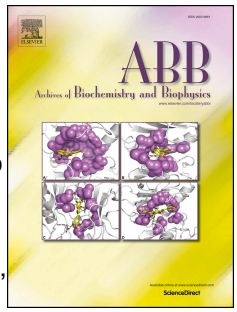

Metabolic switch during adipogenesis: From branched chain amino acid catabolism to lipid synthesis

Anna Halama, Marion Horsch, Gabriele Kastenmüller, Gabriele Möller, Pankaj Kumar, Cornelia Prehn, Helmut Laumen, Hans Hauner, Martin Hrabě de Angelis, Johannes Beckers, Karsten Suhre, Jerzy Adamski

PII: S0003-9861(15)30064-3

DOI: 10.1016/j.abb.2015.09.013

Reference: YABBI 7073

To appear in: *Archives of Biochemistry and Biophysics*

Received Date: 10 May 2015

Revised Date: 13 September 2015

Accepted Date: 15 September 2015

Please cite this article as: A. Halama, M. Horsch, G. Kastenmüller, G. Möller, P. Kumar, C. Prehn, H. Laumen, H. Hauner, M. Hrabě de Angelis, J. Beckers, K. Suhre, J. Adamski, Metabolic switch during adipogenesis: From branched chain amino acid catabolism to lipid synthesis, *Archives of Biochemistry and Biophysics* (2015), doi: 10.1016/j.abb.2015.09.013.

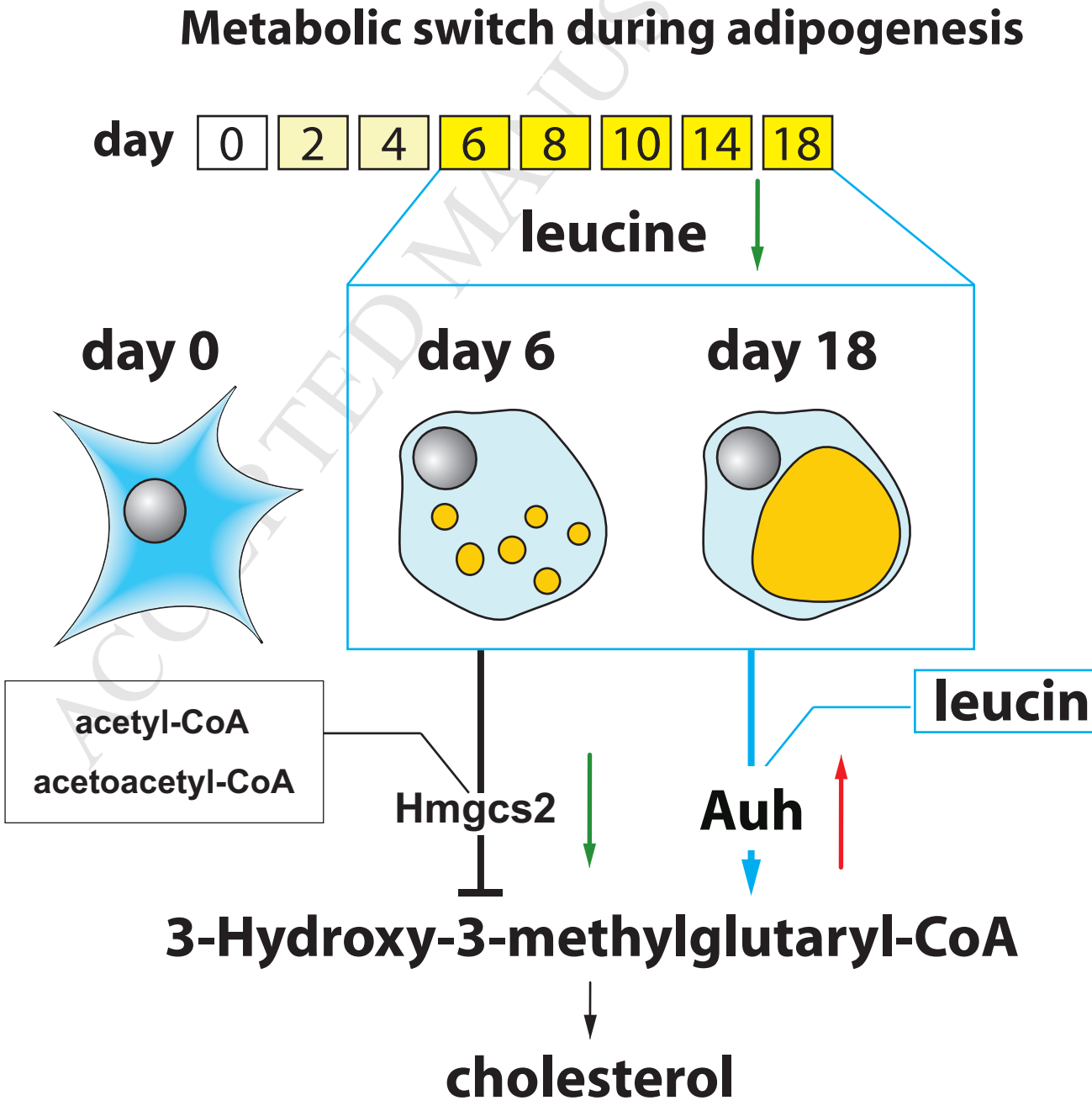

Metabolic switch during adipogenesis: from branched chain amino acid catabolism to lipid synthesis

Anna Halama [1,2,§], Marion Horsch[1], Gabriele Kastenmüller [3], Gabriele Möller [1], Pankaj Kumar [2], Cornelia Prehn [1], Helmut Laumen [4], Hans Hauner [4], Martin Hrabě de Angelis [1,5,6], Johannes Beckers [1,5,6], Karsten Suhre [2], Jerzy Adamski [1,5,6*]

[1] Institute of Experimental Genetics, Genome Analysis Center, Helmholtz Zentrum München, German Research Center for Environmental Health, Neuherberg, Germany

[2] Department of Physiology and Biophysics, Weill Cornell Medical College – Qatar, Doha, Qatar

[§] present address of AH is in Weill Cornell Medical College – Qatar

[3] Institute of Bioinformatics and Systems Biology, Helmholtz Zentrum München, German Research Center for Environmental Health, Neuherberg, Germany

[4] Else Kröner-Fresenius-Centre for Nutritional Medicine, Klinikum rechts der Isar, Technical University München, München, Germany

[5] German Center for Diabetes Research, Neuherberg, Germany

[6] Lehrstuhl für Experimentelle Genetik, Technische Universität München, Freising-Weihenstephan, Germany

* corresponding author

Helmholtz Zentrum München, German Research Center for Environmental Health, Institute of Experimental Genetics, Genome Analysis Center, Ingolstaedter Landstrasse 1, 85764 Neuherberg, Germany, Phone: +49-89-3187-3155, Fax: +49-89-3187-3225

e-mail: adamski@helmholtz-muenchen.de

Metabolic switch during adipogenesis: from branched chain amino acid catabolism to lipid synthesis

Anna Halama [1,2, §], Marion Horsch[1], Gabriele Kastenmüller [3], Gabriele Möller [1], Pankaj Kumar [2], Cornelia Prehn [1], Helmut Laumen [4], Hans Hauner [4], Martin Hrabě de Angelis [1,5,6], Johannes Beckers [1,5,6], Karsten Suhre [2], Jerzy Adamski [1,5,6*]

[1] Institute of Experimental Genetics, Genome Analysis Center, Helmholtz Zentrum München, German Research Center for Environmental Health, Neuherberg, Germany

[2] Department of Physiology and Biophysics, Weill Cornell Medical College – Qatar, Doha, Qatar

[&] present address of AH is in Weill Cornell Medical College – Qatar

[3] Institute of Bioinformatics and Systems Biology, Helmholtz Zentrum München, German Research Center for Environmental Health, Neuherberg, Germany

[4] Else Kröner-Fresenius-Centre for Nutritional Medicine, Klinikum rechts der Isar, Technical University München, München, Germany

[5] German Center for Diabetes Research, Neuherberg, Germany

[6] Lehrstuhl für Experimentelle Genetik, Technische Universität München, Freising-Weihenstephan, Germany

* corresponding author

Helmholtz Zentrum München, German Research Center for Environmental Health, Institute of Experimental Genetics, Genome Analysis Center, Ingolstaedter Landstrasse 1, 85764 Neuherberg, Germany, Phone: +49-89-3187-3155, Fax: +49-89-3187-3225

e-mail: adamski@helmholtz-muenchen.de

Reviewer may access the dataset anonymously at:

http://www.ncbi.nlm.nih.gov/geo/query/acc.cgi?token=yzojmymupvytbyj&acc=GSE34150

Running title: Metabolic pathways in adipogenesis

Abstract

Fat cell metabolism has an impact on body homeostasis and its proper function. Nevertheless, the knowledge about simultaneous metabolic processes, which occur during adipogenesis and in mature adipocytes, is limited. Identification of key metabolic events associated with fat cell metabolism could be beneficial in the field of novel drug development, drug repurposing, as well as for the discovery of patterns predicting obesity risk. The main objective of our work was to provide comprehensive characterization of metabolic processes occurring during adipogenesis and in mature adipocytes. In order to globally determine crucial metabolic pathways involved in fat cell metabolism, metabolomics and transcriptomics approaches were applied. We observed significantly regulated metabolites correlating with significantly regulated genes at different stages of adipogenesis. We identified the synthesis of phosphatidylcholines, the metabolism of even and odd chain fatty acids, as well as the catabolism of branched chain amino acids (BCAA; leucine, isoleucine and valine) as key regulated pathways. Our further analysis led to identification of an enzymatic switch comprising the enzymes Hmgcs2 (3-hydroxy-3-methylglutaryl-CoA synthase) and Auh (AU RNA binding protein/enoyl-CoA hydratase) which connects leucine degradation with cholesterol synthesis and which is strongly regulated during adipogenesis. In addition, propionyl-CoA, a product of isoleucine degradation, was identified as a putative substrate for odd chain fatty acid synthesis. The uncovered crosstalk's between BCAA and lipid

metabolism during adipogenesis might contribute to the understanding of molecular mechanisms of obesity and have potential implications in obesity prediction.

Keywords: adipogenesis, obesity, metabolomics, metabolic pathways, phosphatidylcholines, fatty acids, glycerophospholipids, branched chain amino acids

1 Introduction

Obesity has been identified as a major risk factor for chronic diseases, such as cardiovascular disease, hypertension, dyslipidemia, hyperglycemia [1], type 2 diabetes, insulin resistance [2,3], and some types of cancer [4] including colon [5], breast [6] and prostate cancer [7], as well as an increased risk of premature death [8]. Thus, identification of markers predicting the risk of obesity as well as determination of drug targets could strongly benefit health system. Studies on obesity have recognized several factors including genetic background [9], interplay between environment and genetics [10] as well as epigenetic mechanisms [11] to be associated with this multifactorial disorder. Further understanding of obesity and its co-morbidities could be provided by metabolomics, enabling a global overview on metabolic processes in the body, which simultaneously reflect the sum of gene expression, protein abundance and environmental influence [12]. Lately, metabolomics applied to human cohort for the investigation of the metabolic difference between obese and lean individuals revealed a possible origin of insulin resistance associated with obesity [13]. This study highlighted that an increase in plasma branched chain amino acid (BCAA) concentrations is a hallmark of adult obese individuals. The BCAAs have also been shown to contribute to obesity-associated insulin resistance [13]. In contrast, a study with obese children and children with type 2 diabetes indicated down-regulation in the plasma BCAAs levels compared to healthy lean subjects [14,15]. Clearly, BCAA metabolism is altered in obesity; however, our current understanding how it is regulated and cross-linked to other pathways has not been fully elucidated.

This discrepancy could be associated with the dynamics of fat cell turnover [16]. It has been shown that the number of fat cells is settled during childhood and adolescence and is constant in adulthood of lean and obese individuals, independent of weight loss or gain

[16]. Consequently, differences in fat cell fates of children/adolescents and adults could have direct impact on the diverse patterns in their metabolism, since adipocytes are involved in synthesis and secretion of several hormones [17] and thereby contribute to energy homeostasis [18]. Thus, an increased adipocyte size and/or number results in an increase of molecules released by adipocytes including e.g. adipokines, free fatty acids, and inflammatory mediators, which affect other tissues such as liver, muscle, or neural connections leading to co-morbidities of obesity [3,19].

Exploration of ongoing metabolic changes during adipogenic cell differentiation and in mature adipocytes might facilitate identification of metabolic pathways and biomarkers useful for obesity prediction and identification of novel drug targets.

However, possibilities to perform mechanistic and functional analyses in the whole organism are limited, and therefore we and others applied analyses on the molecular basis of adipogenesis in cell culture.

The adipogenic cell differentiation process has been already investigated with different omics tools, particularly transcriptomics [20-22] and proteomics [23-25] and recently metabolomics [26]. However, more specific insight into the regulation of metabolic pathways can be gained by combining different omics technologies. For example, metabolomics and genomics have already been successfully applied by us in human studies (mGWAS) [12,27-29] and generated new hypotheses for biomedical and pharmaceutical research [29].

In the present study we combined for the first time-metabolomics and transcriptomics in order to provide a comprehensive overview on adipogenesis and fat cell metabolism using the murine 3T3-L1 cell culture model. Our main goal was to reveal interconnected pathways and biomarkers for adipogenesis, to further facilitate the identification of targets useful in prediction and therapies of obesity.

We found associations between BCAA degradation products and intermediates of the cholesterol synthesis as well as even and odd chain fatty acid metabolism. The metabolic signatures of adipogenesis, observed in our study further support the BCAAs as important players in fat metabolism, and highlight odd-chain fatty acids and glycerophospholipids as novel biomarkers of adipogenesis.. Furthermore, differences in BCAA metabolism between children/adolescence and adults, observed previously [13-15], might be associated with process of adipogenesis [16]. Therefore, decreased BCAA level in children might suggest increased formation of the fat cells and simultaneously serve as a biomarker for obesity prediction. The metabolic pathways of BCAAs catabolism and glycerophospholipids synthesis should be considered as potential drug targets preventing obesity.

2 Materials and methods

2.1 3T3-L1 preadipocyte culturing and differentiation into adipocytes

3T3-L1 cells (murine preadipocytes) obtained from the American Type Culture Collection (ATCC) were grown at 37 °C in a 5 % CO_2 humidified atmosphere in growth medium DMEM (High Glucose (4.5 g/L); PAA Laboratories), supplemented with 10 % fatal bovine serum (FBS; PAA Laboratories), 100 IU/mL penicillin, and 100 mg/mL streptomycin (Invitrogen). Cells were cultivated in 6-well plates.

Cells were seeded out in 6-well plates at a density of 8 x 10^4 cells/well and were grown for 2 days until they reached confluence. At day 2, after cells reached confluence (specified as day 0 of adipogenesis or preadipocyte status) adipogenic cell differentiation was induced by cells treatment for four days with a mixture containing

growth medium, insulin (10 mg/mL; Sigma), dexamethasone (1 µM, Sigma), and 3-isobutyl-1-methylxanthine (IBMX; 0.5 mM; Sigma). After four days of differentiation, adipocyte maturation was initiated by cultivating the cells from thereon in growth medium containing only insulin (10 mg/mL) for the remaining maturation process. The media were exchanged every 48 h with fresh media modified as described above. The cells were maintained for 18 days, and samples (cells and their conditioned media separately) were collected at 8 different time points (day 0, 2, 4, 6, 8, 10, 14, and 18).

2.2 Cell harvesting and medium sampling

2.2.1 Medium sampling and cells harvesting for metabolomics

The conditioned medium was removed from the cells and transferred to 1.5 mL reaction tubes, snap-frozen in liquid nitrogen, and stored at -80 °C until further processing.

In order to determine the best method for cell harvesting and metabolite extraction, we examined two harvesting methods including trypsinization and scraping, followed by extraction with three different extraction solvents including water, 40 % MeOH or 80 % MeOH.

For cell harvesting by trypsinization culture medium was removed, cells were washed once with 2 mL of PBS and incubated with 0.5 mL/well of trypsin (Gibco) for 1 min at 37°C. To each well 1.5 mL of medium was added, cells were suspended, transferred to 1.5 mL reaction tubes and centrifuged. The supernatant was removed and cells were washed twice with 1 mL pre-warmed PBS buffer (37 °C). After PBS was aspirated 350 µL of extraction solvent (either water, 40 % MeOH, or 80 % MeOH) were added and samples were snap-frozen in liquid nitrogen and stored at -80 °C until further processing.

For cell harvesting by scraping culture medium was aspirated and cells were washed twice with 2 mL pre-warmed PBS buffer (37 °C). After PBS was aspirated 350 µL of extraction solvent (either water, 40 % MeOH, or 80 % MeOH) were added and cells were scraped off the well bottom in extraction solvent. The suspension (cells in extraction solvent) was transferred to 1.5 mL reaction tubes, snap-frozen in liquid nitrogen and stored at -80 °C until further processing.

After having compared the metabolic profiles of cells harvested by trypsinization and by scraping followed by extraction with either water, 40 % MeOH or 80 % MeOH (Suppl. Fig. 1), we found scraping combined with the 80 % methanol extraction to result in the best detection of metabolites over all metabolite classes (Suppl. Fig 1). This sampling/extraction technique was from then on applied to all cells that were sampled for metabolomics measurements in this study. Samples for metabolomics studies were prepared in triplicates in three independent experiments.

2.2.3 Harvesting of cells for Western blotting

Culture medium was removed, cells were washed once with 2 mL PBS and then scraped off the well bottom with 300 µL lysis buffer (Cell Signalling) supplemented with protease and phosphatase inhibitors (Roche) as well as phenylmethanesulfonylfluoride (PMSF), a serine protease inhibitor. Cell lysates were stored at -80° C until use. Samples for Western blotting were prepared in three independent experiments.

2.2.4 *Harvesting of cells for RNA extraction*

Culture medium was removed, cells were washed once with 2 mL PBS followed by addition of Trizol (0.5 mL/well) and cells were scraped off the well. Cell/Trizol suspensions were transferred to 1.5 mL reaction tubes and stored at – 80 °C until further processing. Samples for RNA extraction were prepared in three independent experiments.

2.3 Oil red O assay

At each harvesting point, medium was removed and cells were incubated for 10 minutes with 3 mL of freshly prepared 10 % formaldehyde at room temperature (RT). After the formaldehyde was removed, cells were washed with 60 % isopropanol and incubated with 1 mL of Oil red O solution (Sigma) at RT for 10 min. The lipid droplet accumulation was analysed under the microscope (Axiovert, Zeiss) and documented using the AxioVision software (Zeiss). The Oil Red O assay was performed in duplicates in three independent experiments.

2.4 RNA isolation, quantitative real-time PCR (qPCR), and gene expression profiling

Total RNA was extracted from cells using the RNeasy Mini kit (Qiagen) according to the manufacturer's protocol. Synthesis of cDNA, required for qPCR, was performed by using the First Strand cDNA Synthesis Kit (ThermoScientific) and following the manufacturer's protocol. Total RNA of 1µg each was reverse transcribed using the oligo(dT)18 primer, included in the kit. For gene expression profiling 500 ng of total RNA per sample was amplified using the Illumina TotalPrep RNA Amplification kit (Ambion).

Quantitative real-time PCR was performed in triplicates in two independent experiments in 384-well plates (ThermoScientific) on a TaqMan 7900HT cycler (Applied Biosystems) equipped with the SDS2.3 software (Applied Biosystems). Primers for the amplification and quantification of *Pparg* were previously described [30]. All other primers were newly designed by using the software Primer3 (http://biotools.umassmed.edu/bioapps/primer3_www.cgi) [31]. Primers were synthesized by Metabion and are listed in Table 1.

The amplification was performed as follows: denaturation at 95 °C for 10 min, 39 amplification and quantification cycles with 95 °C for 15 sec and 60 °C for 1 min, and finally a melting curve program (95 °C for 15 sec, followed by 60 - 95 °C with a heating

rate of 0.1 °C/sec). Signals were detected by fluorescence. The cycle threshold (CT) value was determined by the SDS2.3 software as the cycle at which the fluorescence rose markedly above the background fluorescence.

Relative gene expression was calculated using the comparative $2^{-(\Delta\Delta CT)}$ method [32] and data were normalized to the housekeeping gene importin 8 (Ipo8; in pre-experiments tested to be suited) and the gene expression of samples at day 0 of adipogenic cell differentiation.

Gene expression profiling was conducted as previously described [33,34] using Illumina Mouse Ref-8 v2.0 Expression BeadChips, using 500 ng cDNA per sample. Samples from 8 time points (days 0, 2, 4, 6, 8, 10, 14, and 18) were analysed in three biological triplicates (except time point day 4 in duplicate). Data normalisation (quantile algorithm) and background corrections were performed with the Illumina GenomeStudio 2011.1 software. Significant Analysis of Microarrays (SAM) was applied [35-37] to identify differential gene expression at seven time points (days 2, 4, 6, 8, 10, 14, and 18) compared to day 0 (n=23) . Two to three biological repetitions per time point were assigned to separate groups and genes were considered as differentially regulated when the statistical analysis indicated a significant regulation in at least two of seven time points (fold change > 1.8, FDR < 10%). Cluster analysis was performed using self organising tree algorithm (SOTA) [38] to identify groups of genes with similar expression patterns across the time course (growth termination criteria = 5 cycles). As distance function the Pearson correlation coefficient and the average distance were chosen. Expression data were submitted to the public repository database GEO [39] (identifier: GSE34150).

2.6 Western blotting

Cells collected in lysis buffer were lysed by three freeze-thaw cycles, and proteins were denatured by incubation with 4x Laemmli buffer at 95 °C for 10 min. After separation by

PAGE, proteins were blotted onto a PVDF membrane using a semi-dry blotting apparatus of Bio-Rad. The proteins of interest were detected using primary antibodies against β-Actin, Pparγ, C/ebpβ and C/ebpα from Santa Cruz and appropriate secondary HRP-conjugated antibodies (Dianova and Sigma-Aldrich). After ECL detection (Pierce reagent), the images were captured using a Fusion FX7 apparatus (Vilber Lourmat).

2.7 Metabolomics measurement

At the day of experiment, cell suspensions were transferred to Precellys-Glass/Ceramic SK38 tubes (Peqlab) and homogenised in a Precellys24 apparatus (Peqlab) for 20 s at 5500 rpm. After centrifugation at 18.000 x g, 20 µL of the supernatant was used for metabolomics measurements. Conditioned media were directly applied to kits without any pre-treatment.

Metabolite concentrations were determined in the cells (extracts) and conditioned media. Three different targeted metabolomics assays from Biocrates Life Sciences AG (Innsbruck, Austria) were applied. The Absolute*IDQ* p180 kit assay was used to quantify up to 188 molecules including amino acids (AAs), phospatidylcholines (PCs), lysoPCs, sphingomyelines (SM), carnitines (Cs), and hexoses (H); this assay was performed in the Helmholtz Zentrum München as described previously [40,41]. Two assays for fatty acid and prostaglandin quantification were performed directly at Biocrates as previously described [42]. The samples for the Absolute*IDQ* p180 kit analyses were prepared in triplicates in three independent experiments. Fatty acids and prostaglandin quantification was performed out of the samples prepared in three independent experiments.

The statistical data analysis was performed with the *meta*P server at the Helmholtz Zentrum München (http;//metabolomics.helmholtz-muenchen.de/metap2/), which

provided automated and standardised data analysis for metabolomics data [43]. Self-organising tree algorithm (SOTA) cluster analysis [38] was applied on the fold changes of metabolite concentrations relative to day 0 to identify groups of metabolites with similar patterns across the time course (growth termination criteria = 5 cycles). As distance function the Pearson correlation coefficient and average distance were chosen. Functional data analysis was performed with Ingenuity Pathway Analysis (IPA; Qiagen; http://www.ingenuity.com/products/ipa) as well as Kyoto Encyclopedia of Genes and Genomes (KEGG; http://www.genome.jp/kegg/).

3 Results

3.1 Metabolomics combined with transcriptomics: a comprehensive tool to study adipogenesis

In order to monitor changes occurring at different stages of adipogenesis, we differentiated 3T3-L1 cells for 18 days and collected samples at the 8 time points, namely at day 0, 2, 4, 6, 8, 10, 14, and 18 (the experimental design is presented in Fig. 1A). Differentiation of confluent preadipocytes was initiated by growth medium containing insulin, dexamethasone and IBMX and after day 4 the cells were maturated in medium supplemented with only insulin as described [44]. The accumulation of lipid droplets and the analysis of the transcription factors C/ebpβ, Pparγ, and C/ebpα essential for the regulation of lipid homeostasis [45] on the mRNA and protein levels demonstrated ongoing adipogenesis (results presented in Fig. 1B, C, and D). The two bands observed on the western blot of PPARγ may reflect two isoforms of this protein, which were reported as specific to adipose tissue [46].

Next, metabolomics analyses were performed on both the cells and corresponding conditioned media. Out of the 188 molecules detected by the Absolute*IDQ* p180 kit, 115 metabolites from different metabolic classes (amino acids, carnitines, biogenic amines, hexoses and phospholipids) were quantified and used for further analysis. In the first place we verified whether metabolic alterations have biological background (are correlating with time course) or technical background (are correlating with sample preparation) by using Kendall correlation test. As shown in Suppl. Fig. 2 metabolic alterations were dependent on the adipogenic cell differentiation but not caused by the sample preparation procedure.

In order to reveal a structure in our metabolic data we applied the principal component analysis (PCA) for both conditioned medium and the cells. The PCA plots clearly demonstrated the differences between examined days of adipogenesis (Fig. 2A). Furthermore, PC1 and PC3 strongly reflected the time course of adipogenesis from undifferentiated cells through adipogenic differentiation to mature adipocytes. A tight clustering of biological replicates in both conditioned medium and cells indicates high similarity among the samples from the same time point. We further applied a bidirectional cluster analysis on the fold changes (in relation to preadipocytes (day 0)) of cellular metabolite concentrations to identify clusters of metabolites. The heatmap presented in Fig. 2B showed on the one hand clusters of sample replicates, reflecting the same patterns as were seen in the PCA plots (days of cell differentiation/maturation), and on the other hand six clusters of metabolites. Metabolites grouped in cluster I and II showed down-regulation in the differentiation phase (days 2 – 6) and up-regulation in the maturation phase. In this cluster we found the majority of phospholipids, and short chain carnitines, carnitine, as well as three amino acids namely asparagine, aspartic acid, and glutamine. Metabolites assigned to cluster III - VI were up-regulated during the differentiation phase (days 2 – 6) and displayed down- or no regulation in the maturation phase. In the cluster III phosphatidylcholines and long- as well as medium-chain acylcarnitines were grouped, whereas in cluster VI mainly amino acids were found.

In parallel to metabolomics, we performed transcriptomics by using the Affimetrix Bead technology on cell samples from the 8 time points. The statistical data analysis was performed with the fold changes of gene expression in relation to data for preadipocytes at day 0. We identified 1012 genes significantly regulated in at least 2 of 7 time points (Suppl. Fig. 3). As in case of metabolomics, we applied PCA to reveal a structure in the

transcriptomics data. The PCA analysis of 1012 significantly regulated genes (Fig. 2C) resulted in a pattern similar to that visible in the PCA plot of the cell metabolomics data (Fig. 2A). The PCA of the transcriptomics data was exhibiting clear differences between the days of differentiation and maturation, with simultaneous tight clustering of the replicates. A bidirectional cluster analysis of the regulated genes confirmed the tight clustering of the biological replicates of each time point and enabled grouping of regulated genes into six clusters containing 68 to 375 genes per group (Fig. 2D). Genes in clusters II and V showed uniform up- (cluster V) or down-regulation (cluster II) during the whole period of adipogenesis. Genes of clusters III and IV displayed no changes of expression levels during the first 4 days, but were strongly regulated at later time points. Expression of the genes of clusters I and VI were changed during the first 6 days but were not regulated in comparison to day 0 between days 6 to 8.

The assigned groups of genes were characterized by functional annotations (Fig. 2D). Genes organized in the clusters I – III and VI reflect early molecular events, essential for reprograming of the cell fate, i.e., the change from the fibroblast-like to the fat-accumulating adipocyte. For instance in cluster two, well known signatures of loss of pre-adipocyte-like phenotype namely changes in β- and γ-actin and α- and β-tubulin [47] were found. Furthermore, genes organized in cluster III and belonging to the category 'cellular growth and proliferation' were associated with growth arrest, occurring at early stages of adipogenesis [48]. Genes annotated with 'differentiation of adipocytes, obesity, and adiposity' were highly represented in the clusters II, IV and V. In particular, known attributes of the phenotype of fat cells were found in those groups, like for example the cell death-inducing DFFA-like effector (CIDEC), adipogenin, adiponectin, PPARγ and stearoyl-CoA 9-desaturase (SCD). Because our main objective was to study metabolic processes occurring during adipogenesis and in mature adipocytes we were

interested in genes assigned to the following functional groups: 'oxidation, transport, and uptake of lipids', 'metabolism of cholesterol', 'quantity of ketone body/Ca^{2+}/steroid' and 'metabolism, transport, and uptake of carbohydrate', to complement the metabolic data. By using the IPA software for the analysis of combined metabolomics and transcriptomics data, we were able to elucidate direct links between regulated genes and regulated metabolites as is outlined in the following chapters.~~;~~

Thus, metabolomics data can complement gene expression data and *vice versa*, making pathway analysis more efficient and comprehensive.

3.2 Branched chain amino acids metabolism is strongly regulated during adipogenesis

We were particularly interested in the BCAA metabolism, because previous reports showed discrepancies between the behaviour of those molecules in children/adolescents [14,15] and adult human individuals [13] suffering from obesity, which could be related to the dynamics of fat cell turnover [16]. We reasoned that identification of metabolic pathways connected to the BCAA metabolism could let us understand previously observed differences as well as reveal therapeutic targets or biomarkers enabling obesity prediction.

In our study BCAAs were significantly down-regulated in both condition media and cells (Fig. 3A and B). Thus, in the first place we were screening our data set of 1012 significantly regulated genes for those genes associated with the BCAA metabolism. Figure 3C presents the reconstructed pathway based on metabolomics and gene expression data.

The cells entering the differentiation phase (day 2) exhibited a significant decrease in all BCAA levels (Fig. 3A and B). However, at day 4 an increase of intracellular and significant

decrease of extracellular BCAA levels was observed. The maturation phase (starting at day 6) was characterised by a BCAA decrease in both cells and conditioned medium.

Our results on the metabolite level in cells agreed with the gene expression profiling showing an up-regulation of genes of the BCAA catabolic pathway (Fig. 3C). The up-regulation of the mitochondrial branched chain amino-acid transaminase 2 (*Bcat2*) and down-regulation of the cytosolic *Bcat1* suggested a preferred BCAA-degradation in mitochondria of mature adipocytes. The expression of genes involved in BCAA catabolism reached their maximum exactly at day 6 when all of the BCAAs were significantly down-regulated. Because we used a targeted metabolomics approach, the number of measured metabolites was limited. For instance, 3-hydroxy-3-methylglutaryl-CoA (leucine catabolism), methylmalonate (valine catabolism) and methylmalonyl-CoA (isoleucine breakdown), which are products of the BCAA catabolism, were not measured with our assay. However, genes involved in their synthesis (*Auh*, *Aldh1a7*, and *Pccb)* were strongly up-regulated, which suggests an up-regulation of synthesis of those molecules in the system. We further examined the possible connection of BCAA degradation pathway to other metabolic pathways. Hypothetically, all the above mentioned BCAA breakdown products, can be incorporated into the tricarboxylic acid (TCA) cycle. However, the 3-hydroxymethyl-3-methylglutaryl-CoA lyase (*Hmgcl*), involved in the conversion of 3-hydroxy-3-methylglutaryl-CoA into acetoacetate and acetyl-CoA has not been found among the 1012 significantly regulated genes, which suggest incorporation of 3-hydroxy-3-methylglutaryl-CoA into the steroid metabolism (as speculated in Fig. 3C). In conclusion, the pathway for the catabolism of BCAAs is strongly up-regulated during adipogenesis and in mature adipocytes, suggesting a significant role in fat cell metabolism.

3.3 Leucine degradation products are linked to cholesterol biosynthesis

Based on the above data, we investigated the (possible) connection between the BCAA degradation pathways and other metabolic events occurring during adipogenesis and in mature adipocytes. As shown in Fig. 3C, leucine can be degraded to 3-hydroxy-3-methylglutaryl-CoA, which is one of the intermediates of the cholesterol synthesis pathway. The 3-hydroxy-3-methylglutaryl-CoA synthase (*Hmgcs2*), involved in production of cholesterol-convertible 3-hydroxy-3-methylglutaryl-CoA [49], and 3-hydroxy-3-methylglutaryl-CoA reductase (*Hmgcr*), involved in mevalonate synthesis, are two sequential enzymes in the cholesterol biosynthetic pathway [50]. Interestingly, *Hmgcs2* was up-regulated only from day 0 to day 6 of adipogenesis and downregulated afterwards (Fig. 3A), whereas *Hmgcr* was up-regulated from day 6 until day 18. Simultaneously, the AU RNA binding protein/enoyl-CoA hydratase (*Auh;* also known as methylglutaconyl-CoA hydratase) that is a part of the leucine catabolic pathway and catalyses the synthesis of 3-hydroxy-3-methylglutaryl-CoA, which may serve as product for cholesterol synthesis, was up-regulated starting from day 6 (Fig. 4A). These results indicate a metabolic switch at day 6 (the beginning of the maturation process) in the cholesterol synthesis pathway, which starts to be supplied by the leucine degradation product. As shown in Fig. 4B, 3-hydroxy-3-methylglutaryl-CoA can be incorporated into the cholesterol synthesis pathway through mevalonate, trans-trans-farnesyl diphosphate, dimethylzymosterol, zymosterone and lathosterol. The respective genes involved in the transformation of 3-hydroxy-3-methylglutaryl-CoA into cholesterol were strongly up-regulated (see Fig. 4B). The presented results showed a possible link between leucine degradation and the cholesterol synthesis pathway.

3.4 Interlink between isoleucine degradation and odd chain fatty acid synthesis

We further investigated the catabolic pathway of the two other BCAAs valine and isoleucine. The isoleucine/valine degradation pathway is connected to the citrate cycle (see Fig. 3C), which can supply fatty acid synthesis or/and elongation through acetyl-CoA molecule. Thus, we analysed changes in the fatty acids composition of cells during adipogenesis. Those fatty acids, which were altered during adipogenesis, are presented in Fig. 5. Surprisingly, among the regulated molecules we found only three even chain fatty acids with saturated (Fig. 5A) and unsaturated (Fig. 5B) chains. The majority were odd chain fatty acids with saturated (Fig. 5C) and unsaturated chains (Fig. 5D), which were previously described as not synthesised by mammals, as well as biomarkers of dairy product consumption [51]. Because we used the cell growth medium supplemented with 10% fetal bovine serum and the ruminant animals contain approximately 5 % of odd chain fatty acids in their tissue [52], the increased odd chain fatty acid content in cells may have arisen from the culture medium. Consequently, free odd chain fatty acid concentrations in the conditioned medium were investigated. As shown in Fig. 5E the odd chain fatty acids were up-regulated also in the medium. Thus, odd chain fatty acids seemed to have been net produced by adipocytes and not only taken up from the conditioned medium. There are two possible pathways for odd chain fatty acid synthesis: either the even number fatty acids can undergo alpha-oxidation or alternatively can be de novo synthesised from propionyl-CoA as starting molecule [53]. The genes involved in alpha-oxidation of fatty acids have not been detected in our 1012 significantly regulated genes, therefore we further explored the alternative pathway, namely the synthesis of odd chain fatty acids from the propionyl-CoA molecule. Because isoleucine is catabolized into propionyl-CoA, we suggest a crosslink between isoleucine degradation and odd chain fatty acid synthesis. Indeed, we found propionyl-carnitine

(the transport form of propionic acid) in our metabolite panel to be slightly up-regulated (Fig. 6B), what could be seen as a hint that the isoleucine degradation product propionyl-CoA can possibly be used for *de novo* synthesis of odd-chain fatty acids. Beside, we observed an up-regulation of acetyl-carnitine (transport form of acetic acid) during adipogenesis (Fig. 6A), what supports the suggestion that valine and isoleucine catabolism may support fatty acid elongation or *de novo* fatty acid synthesis by supplying acetyl-CoA (as shown in Fig. 3C). The alteration patterns of e.g. tridecanoic (C13:0) or myristic acids (C14:0) reached their highest peak during the adipocyte differentiation process, followed by a decrease in the maturation phase (Fig. 5A and B). The decrease during maturation might indicate that these molecules are intermediates for elongation processes. Indeed, fatty acids with longer chain length remained up-regulated also during the maturation phase (Fig. 5B and B). The alterations in fatty acid metabolism correlated with the expression of genes involved in fatty acid elongation (*Elovl3*) (Fig. 6C) and desaturation (*Fads2* and *Scd1)* (Fig. 6D). The role of *Elovl3* in elongation of saturated and monounsaturated fatty acid chains containing between 16 and 24 carbons was previously reviewed [54]. Among the genes involved in fatty acid elongation, only *Elovl3* was detected in our gene expression data set. Among the genes, identified in our data set (*Fads1, Fads2, Fads3* and *Scd1)*, which were involved in fatty acid desaturation, only *Fads2* and *Scd1* met the criteria of significant regulation (fold changes higher than 1.5 in relation to day 0). The possible patterns of fatty acid metabolism are presented in Fig. 6E and F. Since fatty acids can be further metabolized to glycerophospholipids (PCs), also these molecules were investigated. The correlation between adipogenesis progression and the accumulation of acyl-acyl (aa) phosphatidylcholines (PCs) and acyl-ether (ae) PCs with an increased saturation number and carbon chain length was observed. The unique, previously not reported

patterns of phosphatidylcholines suggested that during adipogenesis unsaturated fatty acids are incorporated preferentially into the aa PCs (Fig. 7A and C) and elongated fatty acids into the ae PCs (Fig. 7B and D). Collectively, our data show a strong regulation of the fatty acid and the glycerophospholipid metabolism and suggest a link between odd chain fatty acid synthesis and isoleucine degradation, because leucine is a possible main supplier of primer molecules for this pathway.

4 Discussion

Obesity is a highly complex disorder as it arises from the interaction of multiple genes with environmental and behavioural factors, making its prevention and management particularly challenging [55]. Recently, the newly emerging deep-phenotyping technology called metabolomics, which is based on the metabolic profiling of human individuals in large population studies, has enabled the prediction of metabolic diseases before they become clinically incident [56-59]. In addition, the determination of molecules predictive for the development of this complex disease may change current treatment strategies.

Metabolic studies on human obesity have been performed in both obese children [14,15] and adults [13]. However, the reported behaviour of molecules distinguishing the investigated groups (healthy lean children vs obese children and children with type 2 diabetes or healthy lean adults vs obese adults) were not consistent. Increased BCAA levels in obese adults [13] and decreased BCAA levels in obese children and adolescents [14,15] were reported as signatures of obesity. Recently, the dynamics of fat cell turnover during human life was revealed by Spalding et al. [16]. The major factor determining fat mass in human adults is adipocyte number. However the quantity of fat cells remains constant in adults [16] and this amount is established during childhood

and adolescence. Thus, differences in BCAA patterns between children/adolescents and adults could be associated with diverse fat cell metabolism during the life span of individual. Therefore, the investigation of the BCAA metabolism and its link to other pathways, especially during adipogenesis and in mature adipocytes, may provide additional information, which could reveal potential biomarkers predicting obesity and/or novel drug targets.

Here, we combined for the first time metabolomics and transcriptomics to study adipogenesis in an established cell culture model. This experimental design offers a broader view on the metabolism and crosstalk between the metabolic pathways during differentiation and in mature adipocytes. Cells were harvested by scraping instead of by trypsinisation, as recently applied in the metabolic phenotyping of adipogenesis [26], to avoid cell membrane damage [60] and metabolite leakage. We have undertaken precautions to ensure validity of collected samples. The tight clustering of replicates on the PCA plots of both metabolomics and transcriptomics data is demonstrating high quality of our study.

We found significantly regulated metabolites correlating with differentially expressed genes, which exhibited characteristic patterns for different stages of adipogenesis. Our studies are in good agreement with previous reports on transcriptomics [20-22] and metabolomics [26] of adipogenesis. Furthermore, metabolic alteration of the polyamines putrescine and spermidine (Fig. 1B) are consistent with a recent study highlighting that these molecules are associated with lipid accumulation and adipogenesis [61]. In addition, the decreased palmitoylcarnitine (C16) concentration in the cells (data not shown) is in agreement with a previous study that reported a reduction in carnitine concentrations (nonesterified carnitine, acid-soluble acylcarnitines, and acid-insoluble

acylcarnitines) during adipogenesis [62]. However, previous studies on metabolic changes during adipogenesis did not reveal any regulation in the BCAA metabolism.

We also compared our results with studies on human individuals suffering from obesity, since we reasoned that fat cells have some significant impact on the overall composition of body fluids. We found that some metabolic alterations seen in our cell culture study, such as elevated levels of glutamine, asparagine, and fatty acids including myristic, myristoleic, and palmitoleic acid correspond to the results of a study in obese adult individuals [13]. In contrast, our results regarding BCAA metabolism are not consistent with reports describing an increase in BCAAs as a signature for obese adults. However, the biofluids of children suffering from obesity and type 2 diabetes were characterised by a significant decrease in BCAA concentrations, similar to our current results. Decrease in BCAAs level during adipogenesis, observed in our study, together with previous Spalding's report [16], may explain the discrepancy in the study on BCAA metabolism between children/adolescents and adults. It could be concluded that increased BCAA levels can be considered as a signature of obese individuals, while a decrease point to the formation of new fat cells is limited to occur only in children and adolescents [16]. Therefore, decreases in BCAA level in children can be consider as a biomarker for obesity development..

In a further step, we investigated the involvement of BCAA catabolism products in the cellular metabolic network. We uncovered a novel link between branched chain amino acids and lipid metabolic pathways during adipogenesis and in mature adipocytes. To date, leucine conversion into lipids and sterols was only hypothesised [63]. In this study, we noted that the leucine degradation product 3-hydroxy-3-methylglutaryl-CoA may serve as a substrate for cholesterol biosynthesis. Furthermore, we observed a connection between an increase in isoleucine degradation and the accumulation of odd

chain fatty acids. During metabolic pathway analysis we found that propionyl-CoA, which is a product of isoleucine degradation, might be a substrate for odd chain fatty acid synthesis. Although previous studies have suggested that odd chain fatty acids cannot be metabolised in the human body and are delivered via diet only [51], our study clearly demonstrated that odd chain fatty acids can be produced by adipocytes and accumulate during differentiation. Notably, an enhanced synthesis of odd-numbered long chain fatty acids stimulated by an excess of propionyl-CoA has been found in red cell membrane lipids of patients with propionic acidemia and methylmalonic aciduria, which are disorders of propionate catabolism [64].

In conclusion, the altered patterns of BCAAs presented in the current study are consistent with metabolic data from obese children and adolescents, which may be related to the dynamics of fat cell turnover during human life [16]. We also revealed the potential mechanism involved in the metabolic switch, which links BCAA catabolism with cholesterol synthesis. Therefore, the decreased BCAA concentrations should be further investigated toward their potential role as novel biomarkers determining human obesity development already in children. In this work, we presented a decrease in BCAAs, and accumulation of odd chain fatty acids, and phosphatidylcholines as biomarkers of adipogenesis, thereby suggesting a potential role as biomarkers for obesity prediction.

Acknowledgements

We thank Gabriele Zieglmeier (Helmholtz Zentrum München) for her excellent technical assistance in cell culture. We thank Julia Scarpa, Dr. Werner Römisch-Margl and Katharina Faschinger for support with the metabolomics measurements performed at the Helmholtz Centrum München, Genome Analysis Center, Metabolomics Core Facility.

Support for some of the experiments was provided by the Weill Cornell Medical College in Qatar bioinformatics and virtual metabolomics core, which is funded by the Qatar Foundation.

This study was supported in part by a grant from the German Federal Ministry of Education and Research (BMBF) to the German Center Diabetes Research (DZD e.V.) and by the Helmholtz Alliance ICEMED (grant to JB). The funders had no role in study design, data collection and analysis, decision to publish, or preparation of the manuscript.

5 References

1. Lavie CJ, Milani RV, Ventura HO (2009) Obesity and cardiovascular disease: risk factor, paradox, and impact of weight loss. J Am Coll Cardiol 53: 1925-1932.
2. Flier JS (2004) Obesity wars: molecular progress confronts an expanding epidemic. Cell 116: 337-350.
3. Guilherme A, Virbasius JV, Puri V, Czech MP (2008) Adipocyte dysfunctions linking obesity to insulin resistance and type 2 diabetes. Nat Rev Mol Cell Biol 9: 367-377.
4. Calle EE, Thun MJ (2004) Obesity and cancer. Oncogene 23: 6365-6378.
5. Ma Y, Yang Y, Wang F, Zhang P, Shi C, et al. (2013) Obesity and risk of colorectal cancer: a systematic review of prospective studies. PLoS One 8: e53916.
6. Ligibel J (2011) Obesity and breast cancer. Oncology (Williston Park) 25: 994-1000.
7. Amling CL (2005) Relationship between obesity and prostate cancer. Curr Opin Urol 15: 167-171.
8. Calle EE, Thun MJ, Petrelli JM, Rodriguez C, Heath CW, Jr. (1999) Body-mass index and mortality in a prospective cohort of U.S. adults. N Engl J Med 341: 1097-1105.
9. Stunkard AJ, Sorensen TI, Hanis C, Teasdale TW, Chakraborty R, et al. (1986) An adoption study of human obesity. N Engl J Med 314: 193-198.
10. Speakman JR (2004) Obesity: the integrated roles of environment and genetics. J Nutr 134: 2090S-2105S.
11. Dick KJ, Nelson CP, Tsaprouni L, Sandling JK, Aissi D, et al. (2014) DNA methylation and body-mass index: a genome-wide analysis. Lancet 383: 1990-1998.
12. Adamski J (2012) Genome-wide association studies with metabolomics. Genome Med 4: 34.
13. Newgard CB, An J, Bain JR, Muehlbauer MJ, Stevens RD, et al. (2009) A branched-chain amino acid-related metabolic signature that differentiates obese and lean humans and contributes to insulin resistance. Cell Metab 9: 311-326.
14. Mihalik SJ, Michaliszyn SF, de las Heras J, Bacha F, Lee S, et al. (2012) Metabolomic profiling of fatty acid and amino acid metabolism in youth with obesity and type 2 diabetes: evidence for enhanced mitochondrial oxidation. Diabetes Care 35: 605-611.
15. Wahl S, Yu Z, Kleber M, Singmann P, Holzapfel C, et al. (2012) Childhood Obesity Is Associated with Changes in the Serum Metabolite Profile. Obes Facts 5: 660-670.
16. Spalding KL, Arner E, Westermark PO, Bernard S, Buchholz BA, et al. (2008) Dynamics of fat cell turnover in humans. Nature 453: 783-787.
17. Kershaw EE, Flier JS (2004) Adipose tissue as an endocrine organ. Journal of Clinical Endocrinology & Metabolism 89: 2548-2556.
18. Rosen ED, Spiegelman BM (2006) Adipocytes as regulators of energy balance and glucose homeostasis. Nature 444: 847-853.
19. de Ferranti S, Mozaffarian D (2008) The perfect storm: obesity, adipocyte dysfunction, and metabolic consequences. Clin Chem 54: 945-955.
20. Guo X, Liao K (2000) Analysis of gene expression profile during 3T3-L1 preadipocyte differentiation. Gene 251: 45-53.
21. Ross SE, Erickson RL, Gerin I, DeRose PM, Bajnok L, et al. (2002) Microarray analyses during adipogenesis: understanding the effects of Wnt signaling on adipogenesis and the roles of liver X receptor alpha in adipocyte metabolism. Mol Cell Biol 22: 5989-5999.
22. Billon N, Kolde R, Reimand J, Monteiro MC, Kull M, et al. (2010) Comprehensive transcriptome analysis of mouse embryonic stem cell adipogenesis unravels new processes of adipocyte development. Genome Biol 11: R80.

23. Molina H, Yang Y, Ruch T, Kim JW, Mortensen P, et al. (2009) Temporal profiling of the adipocyte proteome during differentiation using a five-plex SILAC based strategy. J Proteome Res 8: 48-58.
24. Welsh GI, Griffiths MR, Webster KJ, Page MJ, Tavare JM (2004) Proteome analysis of adipogenesis. Proteomics 4: 1042-1051.
25. Ye F, Zhang H, Yang YX, Hu HD, Sze SK, et al. (2011) Comparative proteome analysis of 3T3-L1 adipocyte differentiation using iTRAQ-coupled 2D LC-MS/MS. J Cell Biochem 112: 3002-3014.
26. Roberts LD, Virtue S, Vidal-Puig A, Nicholls AW, Griffin JL (2009) Metabolic phenotyping of a model of adipocyte differentiation. Physiol Genomics 39: 109-119.
27. Gieger C, Geistlinger L, Altmaier E, Hrabe de Angelis M, Kronenberg F, et al. (2008) Genetics meets metabolomics: a genome-wide association study of metabolite profiles in human serum. PLoS Genet 4: e1000282.
28. Illig T, Gieger C, Zhai G, Romisch-Margl W, Wang-Sattler R, et al. (2010) A genome-wide perspective of genetic variation in human metabolism. Nat Genet 42: 137-141.
29. Suhre K, Shin SY, Petersen AK, Mohney RP, Meredith D, et al. (2011) Human metabolic individuality in biomedical and pharmaceutical research. Nature 477: 54-60.
30. Fu Y, Luo N, Klein RL, Garvey WT (2005) Adiponectin promotes adipocyte differentiation, insulin sensitivity, and lipid accumulation. J Lipid Res 46: 1369-1379.
31. Rozen S, Skaletzky H (1999) Primer3 on the WWW for general users and for biologist programmers. Methods in molecular biology 132: 365-368.
32. Livak KJ, Schmittgen TD (2001) Analysis of relative gene expression data using real-time quantitative PCR and the 2(-Delta Delta C(T)) Method. Methods 25: 402-408.
33. Kugler JE, Horsch M, Huang D, Furusawa T, Rochman M, et al. (2013) High mobility group N proteins modulate the fidelity of the cellular transcriptional profile in a tissue- and variant-specific manner. J Biol Chem 288: 16690-16703.
34. Horsch M, Schadler S, Gailus-Durner V, Fuchs H, Meyer H, et al. (2008) Systematic gene expression profiling of mouse model series reveals coexpressed genes. Proteomics 8: 1248-1256.
35. Stewart RD, Duhamel TA, Rich S, Tupling AR, Green HJ (2008) Effects of consecutive days of exercise and recovery on muscle mechanical function. Med Sci Sports Exerc 40: 316-325.
36. Saeed AI, Sharov V, White J, Li J, Liang W, et al. (2003) TM4: a free, open-source system for microarray data management and analysis. Biotechniques 34: 374-378.
37. Tusher VG, Tibshirani R, Chu G (2001) Significance analysis of microarrays applied to the ionizing radiation response. Proc Natl Acad Sci U S A 98: 5116-5121.
38. Herrero J, Valencia A, Dopazo J (2001) A hierarchical unsupervised growing neural network for clustering gene expression patterns. Bioinformatics 17: 126-136.
39. Edgar R, Domrachev M, Lash AE (2002) Gene Expression Omnibus: NCBI gene expression and hybridization array data repository. Nucleic acids research 30: 207-210.
40. Römisch-Margl W, Prehn C, Bogumil R, Röhring C, Suhre K, et al. (2012) Procedure for tissue sample preparation and metabolite extraction for high-throughput targeted metabolomics. Metabolomics 8: 133-142.
41. Jourdan C, Petersen AK, Gieger C, Doring A, Illig T, et al. (2012) Body fat free mass is associated with the serum metabolite profile in a population-based study. PLoS One 7: e40009.
42. Unterwurzacher I, Koal T, Bonn GK, Weinberger KM, Ramsay SL (2008) Rapid sample preparation and simultaneous quantitation of prostaglandins and lipoxygenase derived fatty acid metabolites by liquid chromatography-mass spectrometry from small sample volumes. Clin Chem Lab Med 46: 1589-1597.

43. Kastenmüller G, Römisch-Margl W, Wägele B, Altmeier E, Suhre K (2010) metaP-Server: A Web-Based Metabolomics Data Analysis Tool. Journal of Biomedicine and Biotechnology 2011: ID839862.
44. Student AK, Hsu RY, Lane MD (1980) Induction of fatty acid synthetase synthesis in differentiating 3T3-L1 preadipocytes. J Biol Chem 255: 4745-4750.
45. Laxman B, Hall DE, Bhojani MS, Hamstra DA, Chenevert TL, et al. (2002) Noninvasive real-time imaging of apoptosis. Proc Natl Acad Sci U S A 99: 16551-16555.
46. Tontonoz P, Hu E, Graves RA, Budavari AI, Spiegelman BM (1994) mPPAR gamma 2: tissue-specific regulator of an adipocyte enhancer. Genes Dev 8: 1224-1234.
47. Spiegelman BM, Farmer SR (1982) Decreases in tubulin and actin gene expression prior to morphological differentiation of 3T3 adipocytes. Cell 29: 53-60.
48. Gregoire FM, Smas CM, Sul HS (1998) Understanding adipocyte differentiation. Physiol Rev 78: 783-809.
49. Ortiz JA, Gil-Gomez G, Casaroli-Marano RP, Vilaro S, Hegardt FG, et al. (1994) Transfection of the ketogenic mitochondrial 3-hydroxy-3-methylglutaryl-coenzyme A synthase cDNA into Mev-1 cells corrects their auxotrophy for mevalonate. J Biol Chem 269: 28523-28526.
50. Balasubramaniam S, Goldstein JL, Brown MS (1977) Regulation of cholesterol synthesis in rat adrenal gland through coordinate control of 3-hydroxy-3-methylglutaryl coenzyme A synthase and reductase activities. Proc Natl Acad Sci U S A 74: 1421-1425.
51. Wolk A, Furuheim M, Vessby B (2001) Fatty acid composition of adipose tissue and serum lipids are valid biological markers of dairy fat intake in men. J Nutr 131: 828-833.
52. Pereira ASC, Santos MVd, Aferri G, Corte RRPdS, Silva SdLe, et al. (2012) Lipid and selenium sources on fatty acid composition of intramuscular fat and muscle selenium concentration of Nellore steers. Revista Brasileira de Zootecnia 41: 2357-2363.
53. Jenkins B, West JA, Koulman A (2015) A review of odd-chain fatty acid metabolism and the role of pentadecanoic Acid (c15:0) and heptadecanoic Acid (c17:0) in health and disease. Molecules 20: 2425-2444.
54. Kopf T, Peer M, Schmitz G (2012) Genetic and Metabolic Determinants of Fatty Acid Chain Length and Desaturation, Their Incorporation into Lipid Classes and Their Effects on Risk of Vascular and Metabolic Disease. In: Suhre K, editor. Genetics Meets Metabolomics: Springer New York. pp. 191-231.
55. Yang W, Kelly T, He J (2007) Genetic epidemiology of obesity. Epidemiol Rev 29: 49-61.
56. Wang TJ, Larson MG, Vasan RS, Cheng S, Rhee EP, et al. (2011) Metabolite profiles and the risk of developing diabetes. Nat Med 17: 448-453.
57. Floegel A, Stefan N, Yu Z, Muhlenbruch K, Drogan D, et al. (2013) Identification of serum metabolites associated with risk of type 2 diabetes using a targeted metabolomic approach. Diabetes 62: 639-648.
58. Wang-Sattler R, Yu Z, Herder C, Messias AC, Floegel A, et al. (2012) Novel biomarkers for pre-diabetes identified by metabolomics. Mol Syst Biol 8: 615.
59. Ferrannini E, Natali A, Camastra S, Nannipieri M, Mari A, et al. (2012) Early Metabolic Markers of the Development of Dysglycemia and Type 2 Diabetes and Their Physiological Significance. Diabetes.
60. Batista U, Garvas M, Nemec M, Schara M, Veranic P, et al. (2010) Effects of different detachment procedures on viability, nitroxide reduction kinetics and plasma membrane heterogeneity of V-79 cells. Cell Biol Int 34: 663-668.
61. Ishii I, Ikeguchi Y, Mano H, Wada M, Pegg AE, et al. (2012) Polyamine metabolism is involved in adipogenesis of 3T3-L1 cells. Amino Acids 42: 619-626.

62. Cha YS, Eun JS, Oh SH (2003) Carnitine profiles during differentiation and effects of carnitine on differentiation of 3T3-L1 cells. J Med Food 6: 163-167.
63. Rosenthal J, Angel A, Farkas J (1974) Metabolic fate of leucine: a significant sterol precursor in adipose tissue and muscle. Am J Physiol 226: 411-418.
64. Wendel U (1989) Abnormality of odd-numbered long-chain fatty acids in erythrocyte membrane lipids from patients with disorders of propionate metabolism. Pediatr Res 25: 147-150.

Table 1. Primers for qPCR

Mouse gene	Name/Direction	Sequence (5' --> 3')	Tm (°C)
AUH	mAUH_215_for	GGTGCTCGGGATTAACAGAG	60
	mAUH_423_rev	TGGAGACAAAGGGACCAACT	58
C/EBPβ	mC/EBPβ_762_for	GACAAGCTGAGCGACGAGTA	60
	mC/EBPβ _919_rev	AGCTGCTCCACCTTCTTCTG	60
C/EBPα	mC/EBPα _962_for	TGGACAAGAACAGCAACGAGTA	60
	mC/EBPα _1082_rev	GTCAACTCCAGCACCTTCTGT	61
ELOVL3	mELOVL3_133_for	CCCTACCCCAAGCTCTGTAA	60
	mELOVL3_349_rev	CGCGTTCTCATGTAGGTCTG	60
HMGCR	mHMGCR_426_for	GGTATTGCTGGCCTCTTCAC	60
	mHMGCR_562_rev	CTCGCTCTAGAAAGGTCAATCA	60
IPO8	mIPO8_2267_for	CAGCAGGATTGCTTCGAGTA	58
	mIPO8_2434_rev	AGCATAGCACTCGGCATCTT	58
MCEE	mMCEE_457_for	CATCCACTGGGGAGTGATAGT	61
	mMCEE_648_rev	GGGATGGAGGAAAATCACAG	58
MUT	mMUT_377_for	ATTCACACGGGGACCATATC	58
	mMUT_570_rev	CACGAACTCTGGGGTTGTCT	60
MVD	mMVD_37_for	GGGACTCCAGCATCTCAGTTA	61
	mMVD_253_rev	ATGCGGTCCTCTGTGAAGTC	60
PPARγ	mPPARγ_for	TTTTCAAGGGTGCCAGTTT	53
	mPPARγ_rev	AATCCTTGGCCCTCTGAGAT	58

Figure legends

Figure 1. Overview of experimental design and monitoring of adipogenesis

A) Overview of the study design. Murine 3T3-L1 cells were differentiated from preadipocytes to adipocytes over 18 days. Cell and corresponding medium samples of 8 different time points (see squares) were collected and examined as indicated in the workflow. The intensity of yellow color in squares corresponds to the progression of adipogenesis. White – non differentiated cells; light yellow – differentiation phase; dark yellow – maturation phase. Cell differentiation was verified by monitoring the lipid droplet accumulation with Oil red O assay (B) and the photos were taken at initial magnifications ×200. C) The expression patterns of transcription factors *Pparγ, C/ebpβ* and *C/ebpa*, known to promote adipogenesis, were evaluated with quantitative PCR. D) Western blot analyses of PPARγ, C/EBPα and C/EBPβ. The two bands observed for PPARγ reflects its two isoforms. The first band from top reflects PPARγ2 and the second one the PPARγ1.

Figure 2. **Combined metabolomics and transcriptomics enable a broad analysis of adipogenesis.**

We have analysed the transcriptome and the metabolome during adipogenesis in cells. Metabolite measurements were performed with the Absolute*IDQ* p180 kit assay and the transcriptomic analysis using the Illumina BeadChip technology. PCA plots of metabolomics data (A) is based on 115 metabolites in the medium and in cells. The PCA plot of transcriptomics data (C) is based on top 1012 regulated genes. Colour code for days of adipogenesis: red – day 0, orange – day 2, light green – day 4, dark green day 6, light blue - day 8, blue – day 10, dark blue – day 14 and violet – day 18.-Arrows in (A)

and (C) depict the progression of adipogenesis. B) Results of SOTA cluster analysis of the 115 metabolites in cells with the overview on metabolite class in each group. The fold changes are shown on a 0.0 (down-regulation, green) to 2 (up-regulation, red) scale. Gr - group number, Met# - number of metabolites in the group. D) Gene expression profiling at indicated days of adipogenesis. SOTA cluster analysis of the top 1012 regulated genes with the functional assignment of the groups (I-VI) using IPA. Gen# - number of genes in the group. The fold changes are shown on a -5.0 (down-regulation, blue) to 5 (up-regulation, yellow) scale. Table in (B) shows the metabolite class together with number of metabolites in each class and table in (D) shows the gene category/function together with the amount of genes classified.

Figure 3. Catabolic pathway of BCAAs is regulated during adipogenesis.

We have compiled measured data from metabolome and transcriptome analyses for cell samples of 8 different time points (days 0, 2, 4, 6, 8, 10, 14, and 18 of adipogenesis). Metabolite concentrations are shown as boxplots and changes in gene expression levels as bar graphs. Alteration patterns of BCAAs are shown for conditioned medium (A) and cells (B). C) Schematic illustration of BCAA catabolism data including expression data (Illumina Bead Chip data) of indicated genes and concentration data of metabolites (AbsoluteIDQ) along the pathways. Leucine degradation pathway is indicated with blue, valine catabolism with orange and isoleucine breakdown with pink arrows and lines. Grey arrows indicate metabolic pathway which is not a direct part of BCAA breakdown. The expression levels of genes involved in BCAA catabolism are highlighted with bold italic font and metabolites names with bold font. Metabolites not determined in this

study but added for pathway integrity are indicated by bold font without boxplot diagram.

Figure 4. Leucine degradation products are linked into the cholesterol biosynthesis pathway during adipogenesis.

Schematic pathway with data on expression levels of indicated genes. A) Metabolic switch appear at day 6 through the link between leucine degradation and cholesterol biosynthesis. The 3-hydroxy-3-methylglutaryl-CoA synthesis, catalysed by *Hmgcs2* is displaced by expression of *Auh* gene. B) Expression levels of genes involved in cholesterol biosynthesis at different days of adipogenesis. If the gene appears more than once on the schema, the second appearance is highlighted in the red-box instead of duplication of bar plot.

Figure 5. Fatty acids chain composition changes during adipogenesis

A-D) Fatty acids that significantly changed their concentration during adipogenesis are shown; saturated (A) and unsaturated (B) even-chain fatty acids are depicted as well as saturated (C) and unsaturated (D) odd-chain fatty acids. E) Changes of the free fatty acids in the conditioned medium. The characteristic of fatty acids chain is indicated as follows: Cx:y, where x represent the number of chain length and y represents the number of double bounds.

Figure 6. Valine and isoleucine degradation products are linked to the even- and odd- chain fatty acids synthesis during adipogenesis

A) acetylcarnitine and B) propionylcarnitine concentrations might reflect the propionyl-CoA and acetyl-CoA pool during adipogenesis. C) Gene expression patterns of elongase (*Elovl3*) and (D) desaturases (*Scd1* and *Fads2*) at corresponding days of adipogenesis.

Schematic illustration of possible saturation and elongation steps for even (E) and odd (F) chains fatty acids. Selected fatty acids are shown in (E) and (F). The characteristic of fatty acids chain is indicated as follows: Cx:y, where x represent the number of chain length and y represents the number of double bounds.

Figure 7. Metabolic patterns of phosphatidylcholines at different stages of adipogenesis

A-B) Schematic illustration showing significantly altered phosphatidylcholines (PCs) with acyl-acyl (aa) (A) and acyl-ether (ae) (B) chains. PCs highlighted by green frames reflect reactions of increasing desaturation and those marked by blue frames reflect reactions of increasing elongation observed in PCaa and PCae, respectively. C-D) Concentration patterns of selected PC aa and PC ae (D) metabolites in cells during adipogenesis are shown: (C) PC aa metabolites of left green box in (A) are displayed; PCaa with higher double-bond number are more abundant with ongoing adipogenesis. (B) PC ae metabolites of the middle blue box in (B) are displayed; molecules with longer fatty acid chains demonstrate increase in concentration during adipogenesis.

Supplementary information

Suppl. Figure 1. Effect of different harvesting method on metabolite composition.

Concentrations of molecules from different metabolic classes detected after cell scratching (dark colours) or trypsinisation (light colours). Abbreviations: C2 – acetyl-carnitine; C3 - propionylcarnitine; C4 - butyrylcarnitine, Lys - lysine; Phe – phenyl-alanine; Val - valine. For the lipids, only the total compositions of the lipid species are shown. The side chain, substitution region and stereochemistry are unknown. For example PC aa C34:1 indicate phosphatidylcholines (PC) with acyl (aa) side chains containing 34 number of carbons and single double bond in both side chains.

Suppl. Figure 2. Kendall correlation test.

The Kendall correlation between each metabolite concentration and adipogenic cell differentiation (time course) or sample preparation procedure in the medium and cells was determined using the metaP server. The Kendall's tau values were visualised in heat maps. The colours and their intensities are linked to the correlation: green is positive, red is negative and black is no correlation. For best viewing please enlarge this vector graphics.

Suppl. Figure 3. Heatmap of differentially expressed genes during adipogenesis.

List of regulated genes in at least 2 of 7 time points compared to day 0. Fold changes were calculated as ratios of signal intensities of 2-3 biological replicates of each time point and the mean value of the 3 reference samples. The scale bar at the top encoded the log2 fold changes; blue represents down- and yellow up-regulation in the different time points. For best viewing please enlarge this vector graphics.

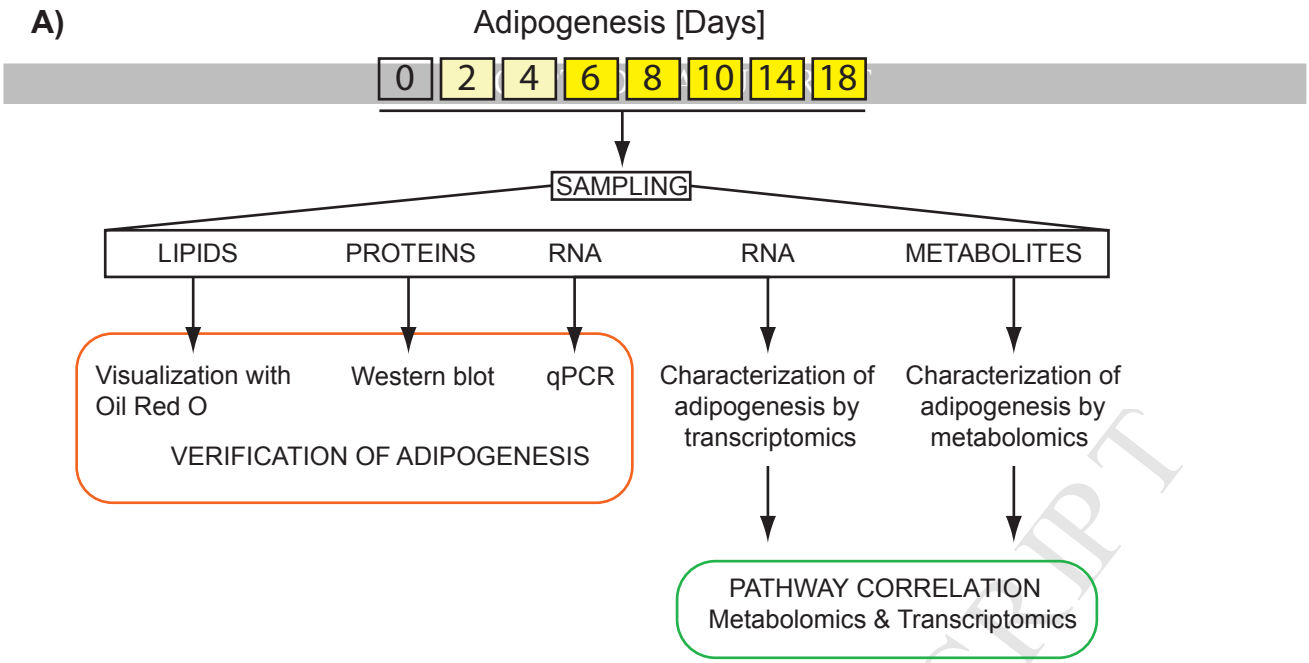

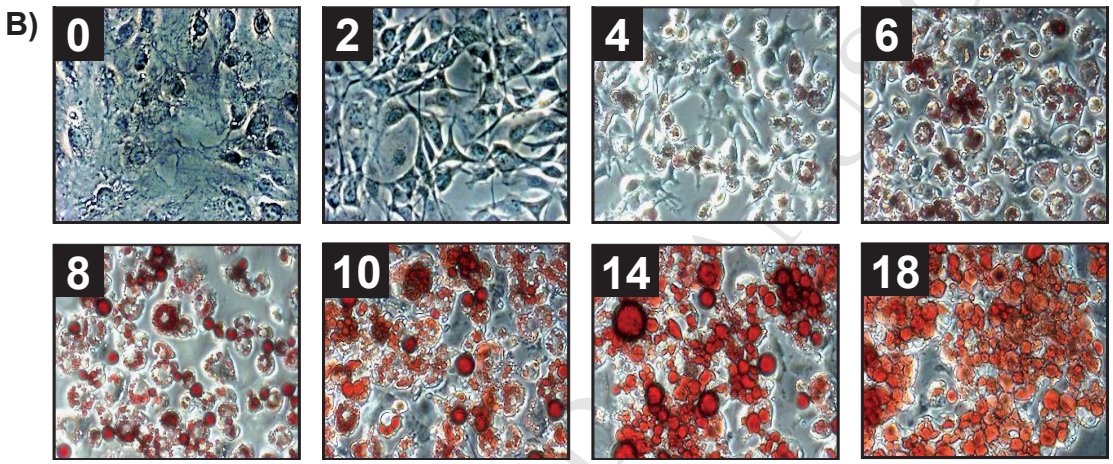

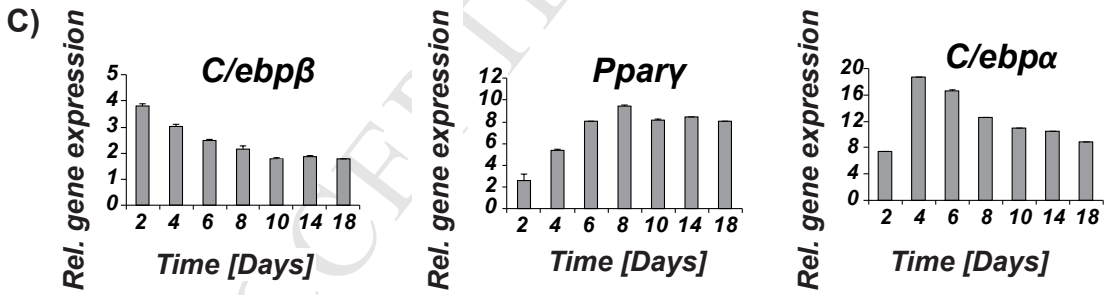

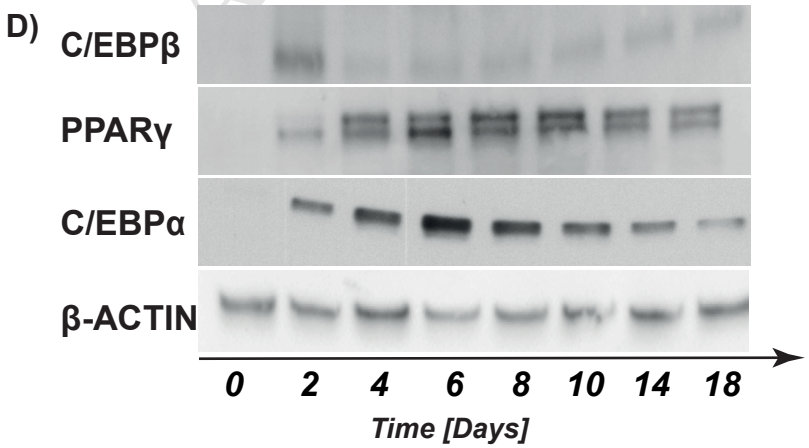

A) Metabolomics PCA

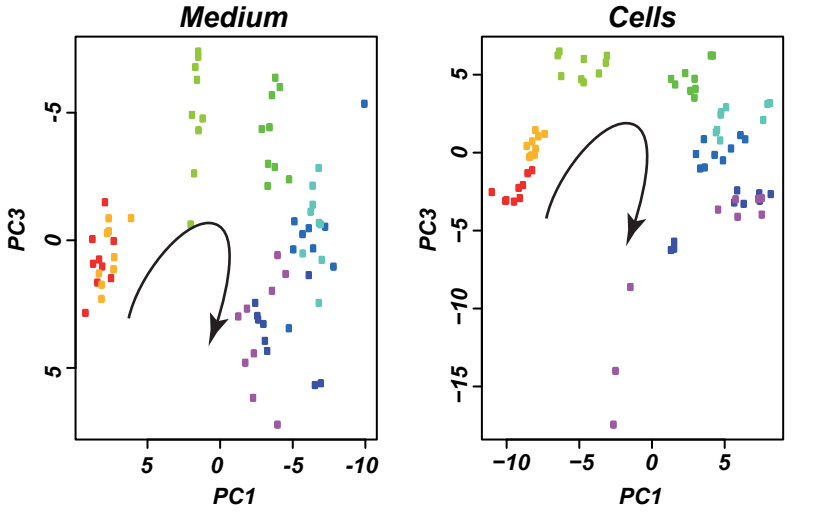

C) Transcriptomics PCA

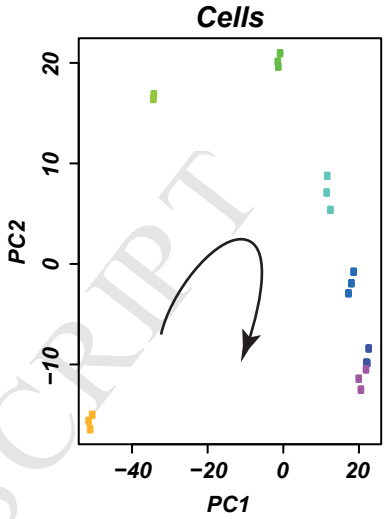

B) Metabolomics fold changes

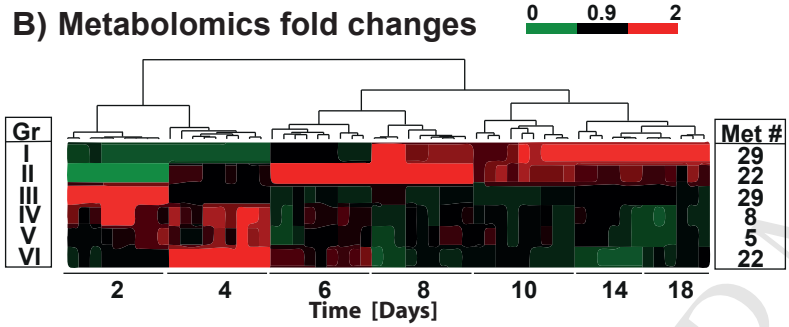

I	Serine Carnitine PC aa (5) PC ae (12) lysoPC (3) SM (7)
II	Amino acid (3) Short-chain acylcarnitine (4) PC aa (6) PC ae (5) lysoPC (4)
III	Putrescine Long- and medium-chain acylcarnitine (6) PC aa (11) PC ae (8) lysoPC (2)
IV	Long-chain acylcarnitine (6) lysoPC (2)
VI	Phenylethylamine Short chain carnitine (4)
VI	Amino acid (17) Hexose Spermidine Creatinine

D) Transcriptomics fold changes

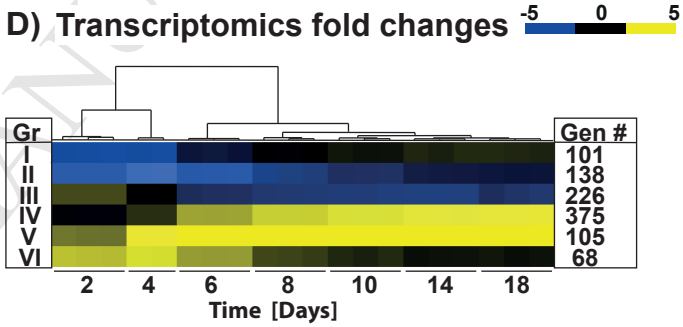

I	Cell proliferation (10) Cell death/viability (20)
II	Cellular movement (45) Organization of cytoskeleton (53) Differentiation of adipocytes (7)
III	Cellular growth and proliferation (59) Gene expression/transcription (46) Cell cycle progression (50)
IV	Adiposity (8) Size of the body (22) Oxidation, transport and uptake of lipids (67) Metabolism of cholesterol (13) Transport of molecules (61) Catabolism of amino acids (26)
V	Adipocyte differentiation/Quantity of adipose tissue (11) Size and mass of adipose tissue (5) lipid concentration and synthesis (18) Quantity of ketone body/Ca^{2+} (6) Metabolism, transport and uptake of carbohydrate (21) Insuline resistance (22) Obesity (13)
VI	Cell cycle (10) Cellular growth and proliferation (19) Differantiation of cells (14)

A) Medium

B) Cell

C)

Leucine

Valine

Isoleucine

Time [Days]

Concentration [µM]

p = 4.4e−11 **

p = 2.4e−06 **

p = 4.2e−10 **

p = 1.1e−10 **

p = 1.3e−10 **

p = 4.7e−11 **

Mitochondrial

Cytosolic

Bcat2

Bcat1

Rel. gene expression

4-Methyl-2-oxopentanoate

3-Methyl-2-oxopentanoic acid

3-Methyl-2-oxobutanoic acid

Dbt

3-Methylbutanoyl-CoA

2-Methylbutanoyl-CoA

2-Methylpropanoyl-CoA

Acads

3-Methylcrotonyl-CoA

2-Methylbut-2-enoyl-CoA

Auh

Methacrylyl-CoA

Aldh1a7

Acaa2

Propionylcarnitine

p= 2.4e−08 **

Methylmalonate

Hmgcs2

3-Hydroxy-3-methylglutaryl-CoA

Methylmalonylcarnitine

p = 1.7e−11 **

Steroid metabolism ?

Hmgcl

Acetoacetatyl-CoA

Acetoacetate

Pccb

Acetylcarnitine

p = 3.2e−10 **

Acetyl-CoA

Citrate cycle

Succinyl-CoA

S-Methylmalonyl-CoA

Mut

Mcee

A)

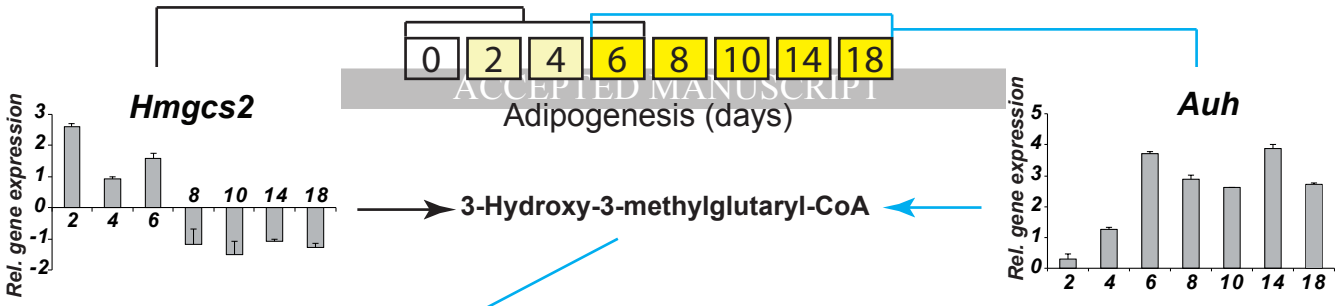

B)

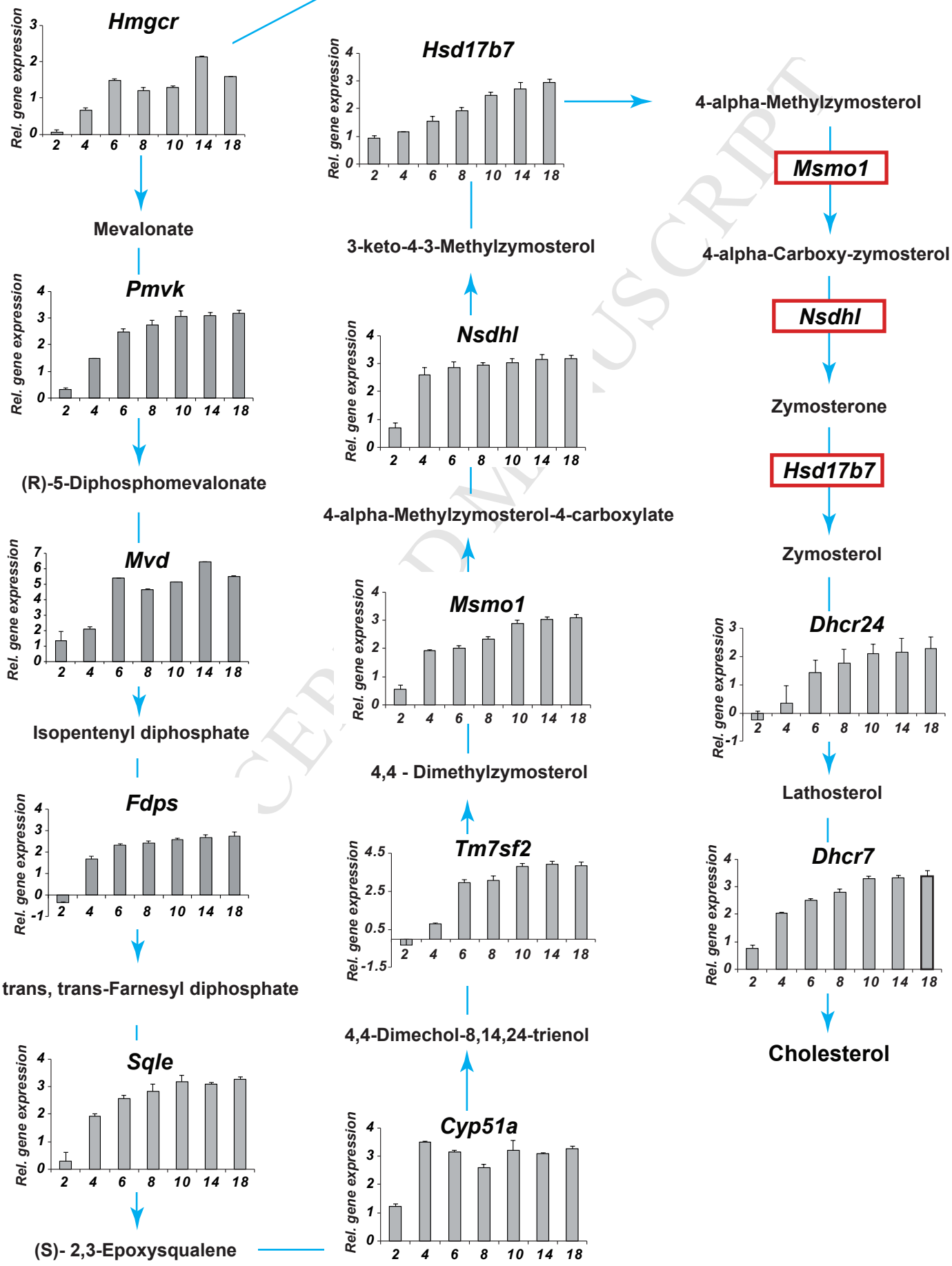

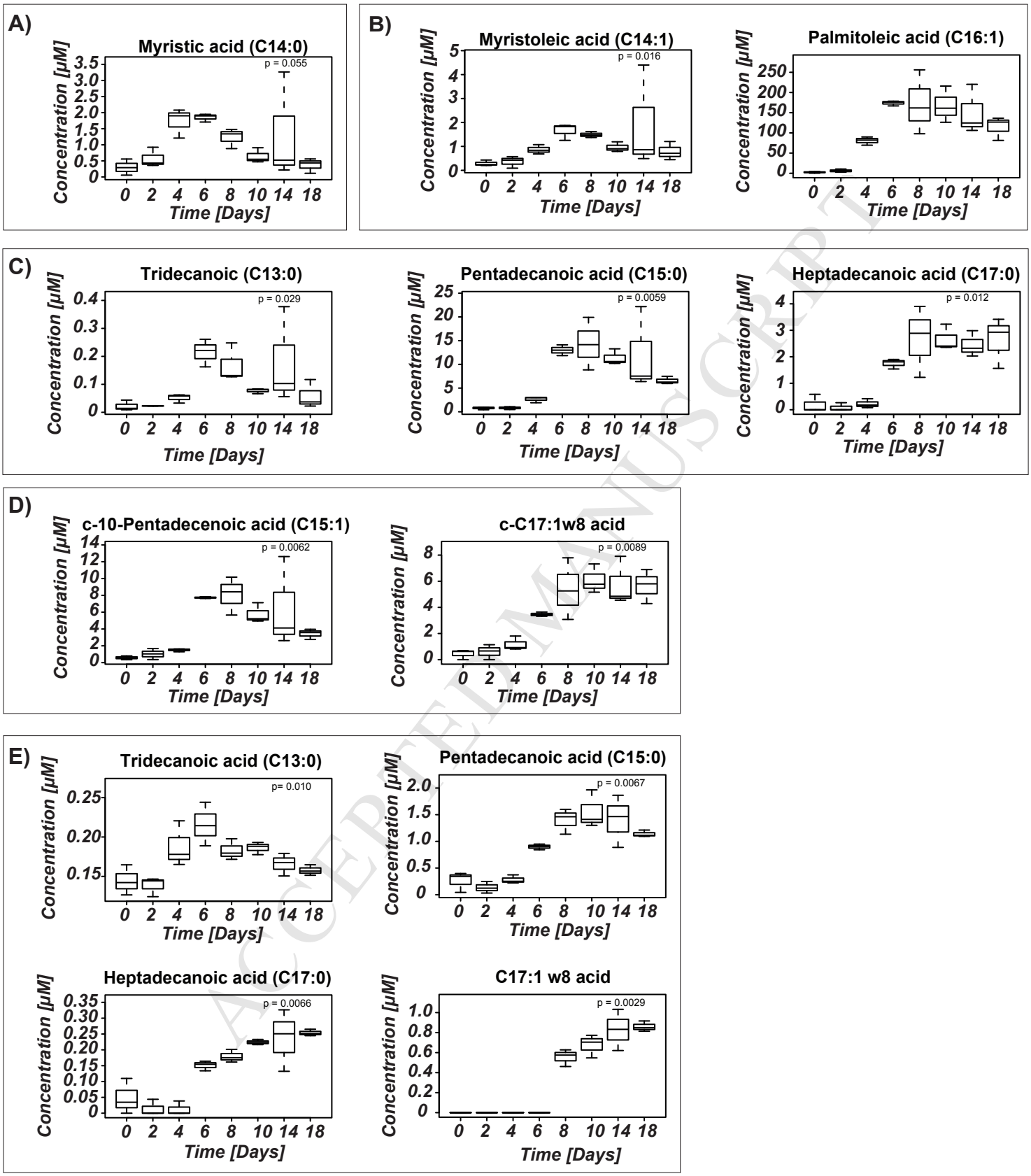

A)

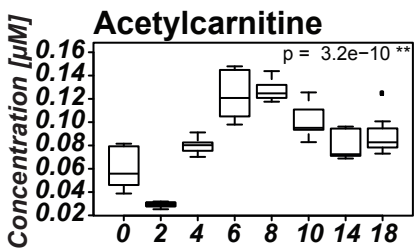

B)

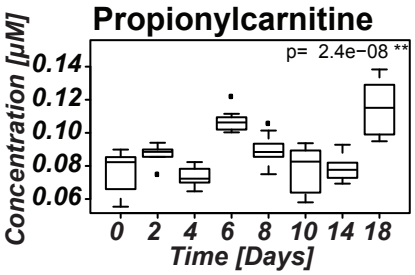

C)

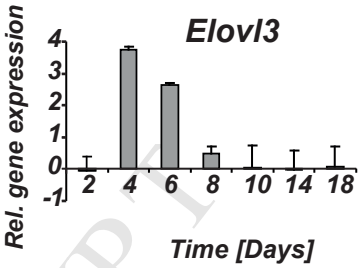

D)

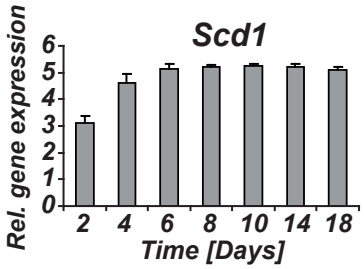

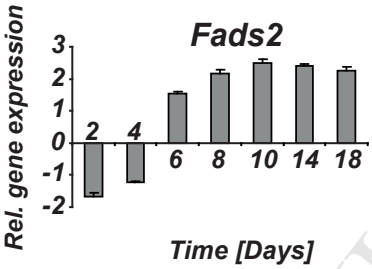

E)

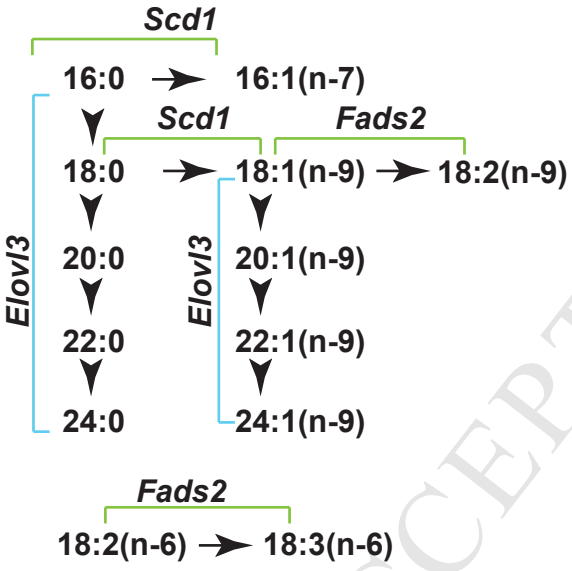

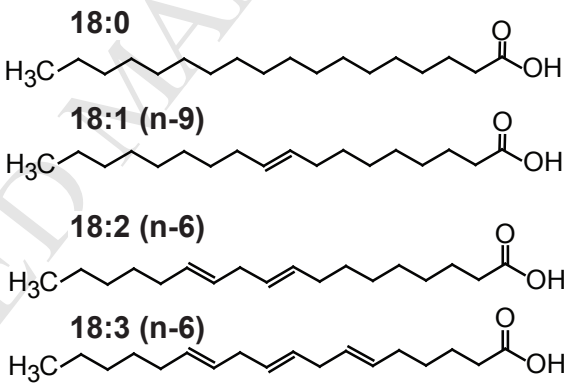

F)

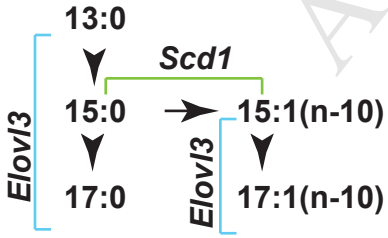

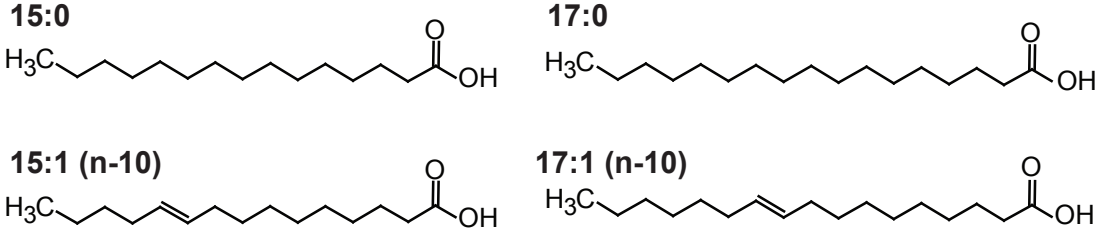

A)

PC aa CX:Y

DESATURATION

30:0	32:0				
	32:1	34:1	36:1		
	32:2	34:2	36:2		
		34:3	36:3	38:3	
		34:4	36:4	38:4	40:4
			36:5	38:5	40:5
				38:6	

B)

PC ae CX:Y

30:0		34:0		38:0	
30:1	32:1	34:1	36:1		
	32:2	34:2	36:2	38:2	
		34:3	36:3	38:3	40:3
		34:4	36:4	38:4	40:4
			36:5	38:5	40:5
				38:6	40:6

ELONGATION

C)

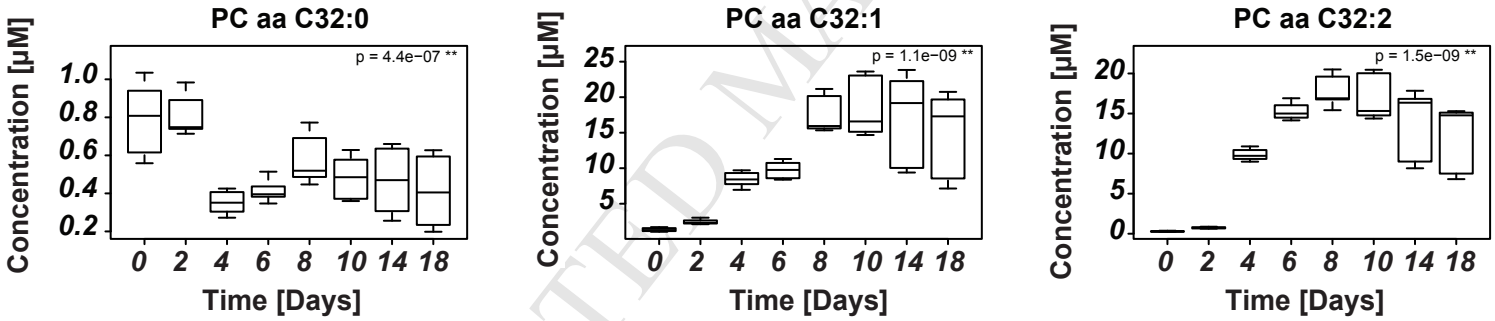

D)

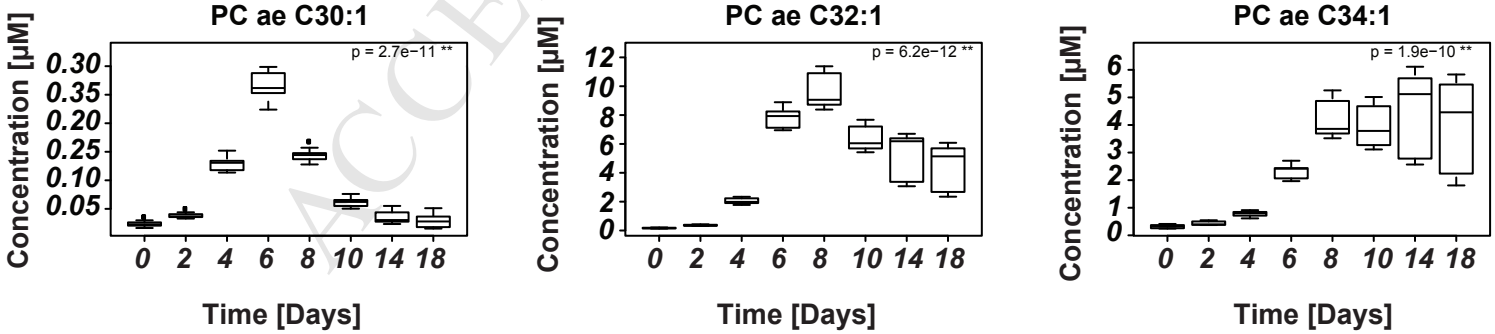

Highlights Halama et al.

- Adipogenesis in cell culture was monitored by transcriptomics and metabolomics
- Multiple lipids and amino acids are regulated in adipogenesis
- Enzymatic switch comprising the enzymes Hmgcs2 and Auh connects leucine degradation with cholesterol synthesis